Bull Volcanol (1996) 58:131–143

ORIGINAL PAPER

K. Kano

A Miocene coarse volcaniclastic mass-flow deposit in the Shimane Peninsula, SW Japan: product of a deep submarine eruption?

Received: 10 January 1996 / Accepted: 23 February 1996

Abstract A subaqueous volcaniclastic mass-flow deposit in the Miocene Josoji Formation, Shimane Peninsula, is 15–16 m thick, and comprises mainly blocks and lapilli of rhyolite and andesite pumices and non- to poorly vesiculated rhyolite. It can be divided into four layers in ascending order. Layer 1 is an inversely to normally graded and poorly sorted lithic breccia 0.3–6 m thick. Layer 2 is an inversely to normally graded tuff breccia to lapilli tuff 6–11 m thick. This layer bifurcates laterally into minor depositional units individually composed of a massive, lithic-rich lower part and a diffusely stratified, pumice-rich upper part with inverse to normal grading of both lithic and pumice clasts. Layer 3 is 2.5–3 m thick, and consists of interbedded fines-depleted pumice-rich and pumice-poor layers a few centimeters thick. Layer 4 is a well-stratified and well-sorted coarse ash bed 1.5–2 m thick. The volcaniclastic deposit shows internal features of high-density turbidites and contains no evidence for emplacement at a high temperature. The mass-flow deposit is extremely coarse-grained, dominated by traction structures, and is interpreted as the product of a deep submarine, explosive eruption of vesicular magma or explosive collapse of lava.

Key words Submarine eruption · Explosive lava collapse · Coarse pumice · Volcaniclastic mass flow · Traction · Suspension

Introduction

This paper describes a coarse-grained submarine volcaniclastic mass-flow deposit and discusses its origin. The deposit occurs in the Early to Middle Miocene Josoji Formation, Shimane Peninsula, SW Japan, and is informally called the Tayu Volcaniclastic Bed E. It contains no evidence that it was deposited from a hot and gas-supported pyroclastic flow, but textural and grain-size evidence suggest that the deposit resulted from a deep submarine, explosive eruption of vesicular magma or explosive lava collapse.

Subaqueous pyroclastic flow deposits are the subaqueous equivalents of subaerial pyroclastic flow deposits (Fiske 1963; Fiske and Matsuda 1964). The term has been applied generally to the mass-flow deposits which are composed mostly of pyroclastic debris and emplaced in subaqueous environments, without reference to the temperature and contained fluid phase of the flow (Fiske 1963; Fiske and Matsuda 1964; Fisher and Schmincke 1984, p. 285). Typically, the deposits comprise a massive, poorly sorted lower division and a parallel-stratified upper division (Fisher 1984) as proposed by Fiske and Matsuda (1964). Some deposits are, however, welded (e.g. Francis and Howells 1973; Howells et al. 1985; Kokelaar and Busby 1992; Schneider et al. 1992), or show magnetic evidence (Kato et al. 1971; Yamazaki et al. 1973; Tamura et al. 1991) or textural evidence (Kano 1990; Cole and DeCelles 1991; Kano et al. 1994) for high-temperature emplacement. Others show lateral and vertical facies changes from debris-flow deposits to turbidites (Tasse et al. 1978; Lajoie 1979) or from high-density turbidites to low-density turbidites (Yamada 1973, 1984; Cole and Stanley 1994) with little evidence of high-temperature emplacement.

Cas and Wright (1987, p. 271, 1991) and Stix (1991) proposed that the term subaqueous pyroclastic flow be used as it is in subaqueous settings to specify a hot, gas-supported pyroclastic density current. Subaqueous water-supported pyroclastic flow deposits were termed volcaniclastic mass-flow deposits (Cas and Wright 1987, p. 271, 1991). This nomenclature does not separate water-supported flows generated directly from eruptions from those stemming from much later sedimentation. Nevertheless, it is still useful and is used in this paper. It is extremely difficult to establish unequivocally an eruption occurring in ancient volcanic successions.

Editorial responsibility: S. Carey

Kazuhiko Kano
Geology Department, Geological Survey of Japan,
1-3, Higashi 1-chome, Tsukuba, Ibaraki, 305, Japan

Geologic setting

The Tayu Volcaniclastic Bed E of the Early to Middle Miocene Josoji Formation crops out at a large sea cliff north of Etomo, Shimane Peninsula, over a distance of several hundred meters (Fig. 1). The exposure includes four black shale beds and six other volcaniclastic mass-flow deposits which are together informally called the Tayu Volcaniclastic Beds A to G in ascending order (Fig. 2). The shale beds are thinly to thickly bedded with sand- to silt-sized volcaniclastic layers several to 20 cm thick. Strata gently dip north as a whole, but locally south at angles of 5–15°.

The Early to Middle Miocene Josoji Formation in and around Etomo conformably overlies shallow freshwater to marine sediments, and comprises mainly black argillaceous rocks, rhyolite water-chilled lavas and intrusive rocks, and volcaniclastic rocks mainly of rhyolite composition. Rhyolite lavas and intrusive rocks form a volcanic pile in the Asahiyama (Asahi Mountain) area a few kilometers south of Etomo. This edifice includes no terrestrial deposits and is flanked by many volcaniclastic mass-flow deposits and black argillaceous rocks (Kano and Nakano 1986; Kano et al. 1988). The mass-flow deposits commonly include coarse rhyolite pumice and lithic clasts up to a few tens of centimeters to 1 m in diameter (Kano and Nakano 1986). Black argillaceous rocks bear benthic foraminifera assemblages indicative of continental shelf to upper bathyal environments (Nomura 1986). Black shales interbedded with the Tayu Volcaniclastic Beds A–G commonly contain authigenic pyrite, but neither foraminifera nor other marine fossils have been found, possibly reflecting an anoxic submarine environment or hydrothermal alteration by adjacent gabbro to diorite intrusions.

The rhyolite edifice in the Asahiyama area is, therefore, likely to have been submerged, and flow directions from the Tayu Volcaniclastic Beds C and D (Kano et al. 1988) suggest that it was the source of the surrounding subaqueous volcaniclastic flow deposits. The upper part of the Tayu Volcaniclastic Bed C shows locally north-dipping cross-stratification, and the shale bed, occurring between the Tayu Volcaniclastic Beds C and D, is slightly thrust northwards (Fig. 2), due probably to the shear imparted from the overlying flow of the Tayu Volcaniclastic Bed D (Kano et al. 1988).

Occurrence

The Tayu Volcaniclastic Bed E is 15–16 m thick, and comprises mainly blocks to lapilli of rhyolite and andesite pumices and non- to poorly vesiculated, plagioclase-phyric glassy rhyolite with minor ash of plagioclase and pumice shreds. Based on the internal structures and constituent materials, this bed can be divided in ascending order into layers 1, 2, 3, and 4 (Figs. 2 and 11).

Constituent materials

Lithic clasts are concentrated mainly in the lower part of the Tayu Volcaniclastic Bed E, and are mostly non-

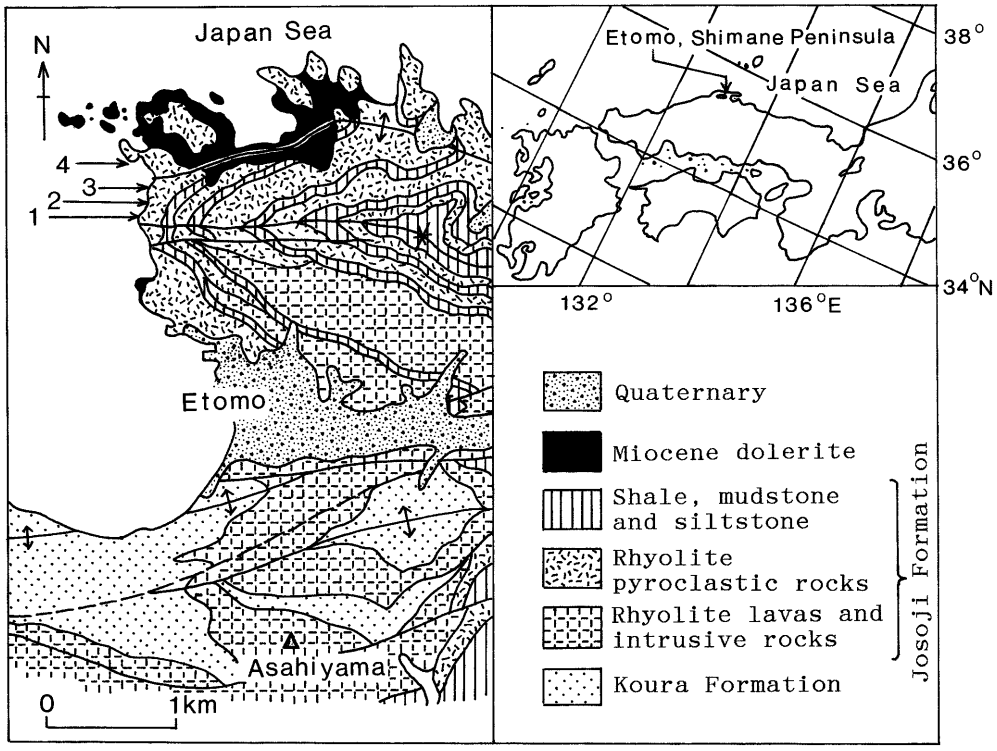

Fig. 1 Geologic map showing the studied outcrop and the locations of geologic columns 1–4 shown in Fig. 2. (Modified after Kano et al. 1988)

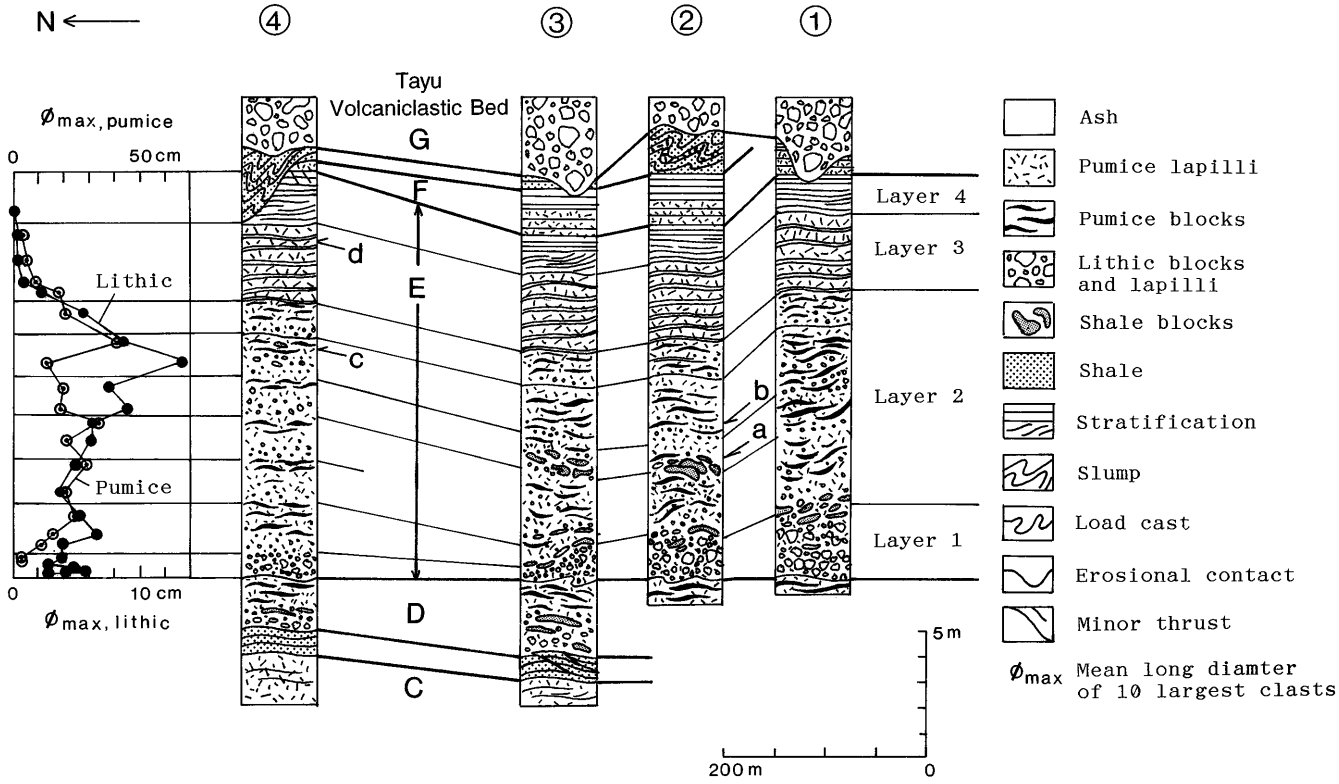

Fig. 2 Geologic columns at locations 1–4 (Fig. 1) showing the internal features of the Tayu Volvaniclastic Bed E. The points *a–d* indicate where the orientation data sets presented in Fig. 7 were collected

to poorly vesiculated, plagioclase-phyric glassy rhyolite. Other lithic clasts include glassy andesite, black shales, sandstone, and tuffaceous rocks. Glassy rhyolite and andesite are entirely replaced by secondary minerals, but glassy parts are recognized as homogeneous domains composed of minute secondary minerals. Most of the lithic clasts are smaller than a few tens of centimeters in diameter, but shale clasts commonly reach a few meters.

Pumice clasts are the most common constituents of the Tayu Volcaniclastic Bed E. They can be classified into two types: pale green pumice and dark green pumice. Pale green pumice is much more predominant than dark green pumice. Although entirely altered to albite, quartz, and clays, the pale green pumice and dark green pumice contain 78–80% SiO_2 and 50–54% SiO_2, respectively, which is thought to reflect differences in the original magma composition. Pale green pumice is partly interstratified with or encloses dark green pumice within single clasts, suggesting mixing of the rhyolite and andesite magmas in the magma chamber or conduit. With both types of pumice, vesicles are commonly compacted, except where filled with albite, chlorite, and quartz, enhancing a fibrous appearance of the pumice. On a visual inspection of the thin sections, dark pumice is more vesicular with a porosity of 70–90%, whereas pale green pumice is less vesicular with a porosity of 60–80%. Some clasts of pale green pumice show flow bands represented by interlayering with non- to poorly vesiculated plagioclase-phyric glassy rhyolite.

Internal structures

Layer 1 is a poorly to moderately sorted, inversely to normally graded lithic breccia (Figs. 2 and 3). The base is sharp and parallel to the underlying bed (Figs. 3 and 4), but locally undulated or folded (Fig. 3B) with E–W trending axial traces and warped with an upward cusp, presumably due to a rapid escape of water from subjacent strata during emplacement (Fig. 4). Lithic clasts, mainly of fine lapilli- to block-sized, subangular to angular rhyolite, occupy 60–80 vol.% of this layer. Black shale clasts up to a few meters in diameter and finer sandstone clasts also occur sporadically.

Layer 1 decreases in thickness over a distance of only approximately 500 m from 3–5 m in the south (at location 1) to 0.3–1 m in the north (at location 4). Although layer 1 contains lesser fines in the north, there is no systematic lateral variation in the maximum size of lithic clasts.

Layer 2 is a tuff breccia to lapilli tuff composed mainly of rhyolite lithic clasts and pumice clasts with minor shale clasts. The base of layer 2 is marked by an abrupt decrease in the volume of lithic clasts (Fig. 3), and commonly undulates with E–W trending crestlines (Fig. 4). The undulation is 0.5–2 m in height and larger than 5 m in length, and is locally overturned northward.

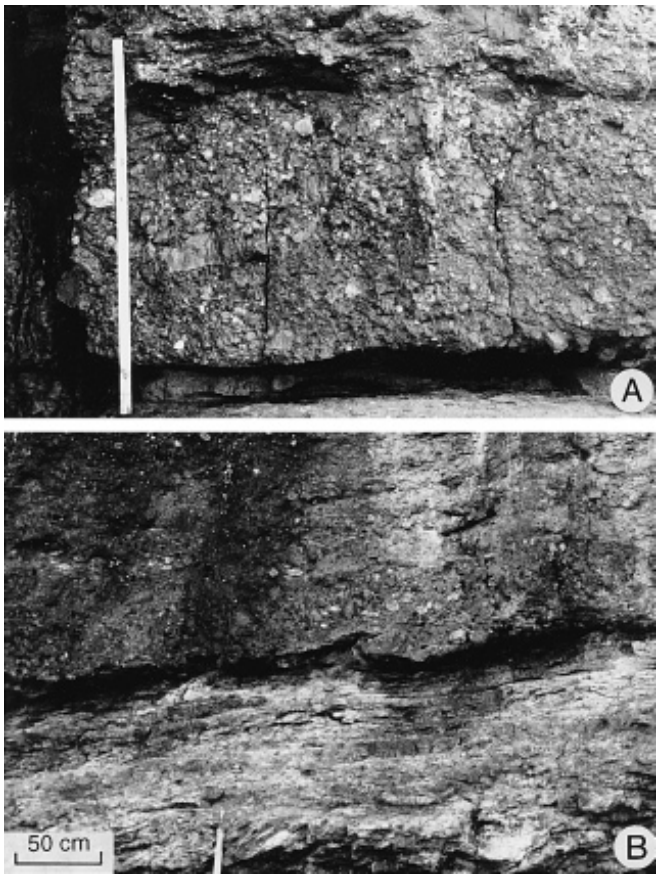

Fig. 3 **A** Inversely to normally graded lithic breccia of layer 1, transitional to the overlying, diffusely stratified and poorly sorted tuff breccia of layer 2 at a place between locations 2 and 3. Shale blocks are common above layer 1. *Scale bar* is 1.8 m long. **B** Sharp base of layer 1 with local syn-depositional folds, underlain by the stratified pumice lapilli tuff of the Tayu Volcaniclastic Bed D at a place between locations 2 and 3

Fig. 4 Undulated top and planar base of layer 1 (lithic breccia) at a place between locations 2 and 3. Wavy stratification at the base of layer 2 (tuff breccia) is discussed in text

Local, parallel to wavy stratification near the base of layer 2 is manifested by thin, lenticular layering of different size populations of lithic and shale clasts (Fig. 4).

Within layer 2, lithic clasts, up to 30 cm in diameter, occupy 10–50 vol.% of the bulk rock, and pumice clasts, up to 5–30 cm in width and 10–200 cm in length, occupy 40–80 vol.%. Coarse pumice blocks occur repeatedly in swarms which are underlain by inversely to normally graded or massive lithic-rich layers (Fig. 2). These pumice blocks are commonly oriented parallel to the layer surface with E–W trending long axes (Fig. 7B, C), representing vague, discontinuous, parallel to wavy stratifications (Figs. 2, 4, and 6).

Tabular to lenticular shale blocks over 2 m long occur locally in swarm parallel to subparallel to the pumice blocks (Fig. 2). These concentrations lie close to the basal part of layer 2 at location 1, but at even higher stratigraphic levels at northern locations (Fig. 2). The short axes of the shale blocks are perpendicular or oblique to the surface of the layer, and their long axes are parallel to the surface of the layer and oriented mainly in an E–W direction (Fig. 7A), similar to the pumice blocks. Coarse shale blocks are folded locally with E–W trending hinges and imbricated southward (Fig. 5) indicating that the flow direction of layer 2 was from south to north.

In the downflow direction layer 2 increases in thickness from 6–8 m to 8–11 m and bifurcates into multiple, but thinner, depositional units which individually comprise a lithic-rich, inversely to normally graded or massive lower part and a pumice-rich, diffusely stratified upper part with locally poorly defined or amalgamated unit boundaries (Fig. 2). Shale and pumice clasts also decrease in maximum size, whereas lithic clasts remain constant, 20–40 cm in maximum size, with no lateral size variation.

Layer 3 is 2.5–3 m thick and consists of interbedded pumice-rich and pumice-poor layers (Fig. 8). This layer is transitional from layer 2, but is more depleted in lithic clasts with an abrupt reduction in the size of both lithic and pumice clasts. Lithic clasts are granule- to coarse-grained sand in size and less than 5 vol.% of layer 3.

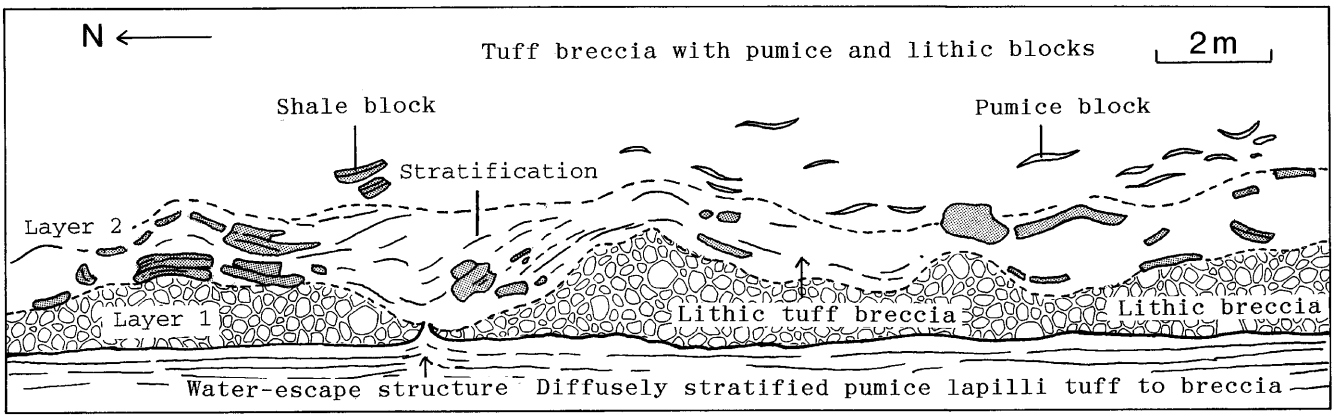

Fig. 5 Imbrication of shale blocks dipping south (to the right of this photo), in the lower part of layer 2, which is 2–3 m thick and underlain by lithic breccia of layer 1 at location 2

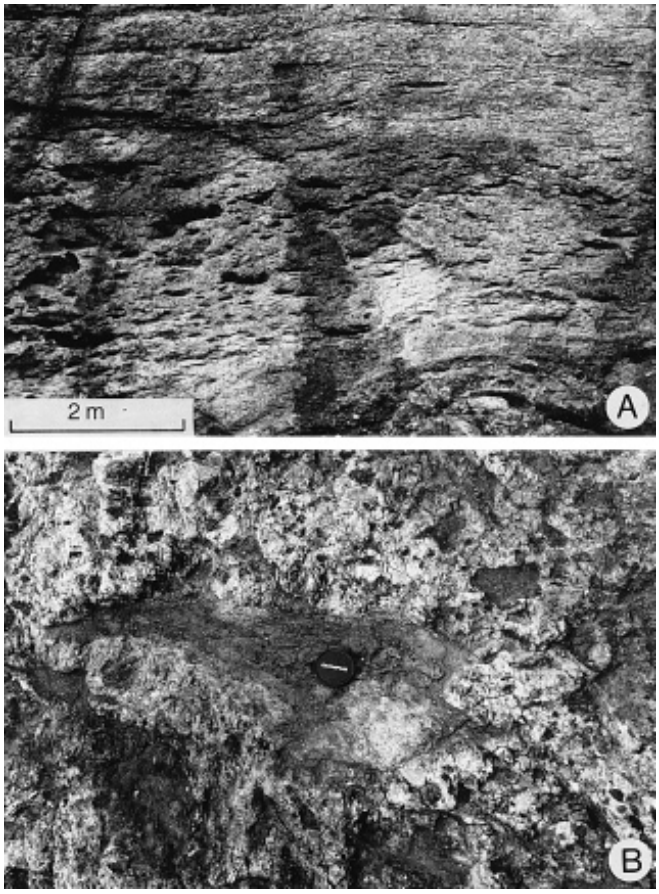

Fig. 6 **A** Upper part of layer 2, 4–5 m thick with a swarm of tabular to lenticular pumice blocks at location 2. A thin unit in the upper part of this photo is interpreted to be another subunit of layer 2. **B** Pumice blocks in the upper part of layer 2 at location 4. *Lens-cap* diameter is 6 cm

Pumice-rich layers in layer 3 are 2–20 cm thick and comprise mainly pumice lapilli 0.5–3 cm wide and 1–6 cm long. Pumice lapilli lie parallel to the layers, with the long axes trending a NE–SW direction (Fig. 7D), which is normal to the long axes of pumice blocks of the underlying layer 2 (Fig. 7B, C). Pumice-poor layers are 1–2 cm thick and consist of very coarse to coarse sand-sized pumice and plagioclase. They commonly show parallel laminae and parting lineations parallel to the pumice alignments in pumice-rich layers (Fig. 7D). Pumice-rich layers become thinner and finer-grained upward, whereas pumice-poor layers remain relatively constant in thickness and grain size.

Layer 4 has a thickness of 1–2 m and comprises mainly well-stratified and well-sorted coarse to fine sand-sized plagioclase, pumice shreds, and lesser amounts of lithic clasts (Fig. 9). The base is sharp, but shows no erosional features. Individual laminae are commonly millimeters to centimeters thick and become thinner and finer upward. They commonly lie horizontally, but are locally cross-stratified in a dune- or antidune-like wavy forms (Fig. 9A). At location 4 the crests strike mainly NWN–SES, and parting lineations and pumice alignments are oriented normally with regard to this strike (Fig. 7D). The flow direction of this layer is therefore from SSW to NNE or from NNE to SSW.

Layer 4 is overlain sharply by the pumice lapilli tuff of the Tayu Volcaniclastic Bed F. This lapilli tuff, together with the upper part of layer 4 of the Tayu Volcaniclastic Bed E, is slumped locally or thrust from SSW to NNE. The thrusts are minor with net slips less than a few centimeters (Fig. 9B). Thrust planes dip south at angles of 30–45° to the original horizontal bedding with strike lines curved convex to a NNE direction. A few rootless clastic dikes occur in layer 4 and slightly intrude into the overlying pumice lapilli tuff (Fig. 9C). They are 1–20 cm wide and 20–30 cm long, stand almost upright, and strike subparallel to parallel to the strikes of the cross-stratifications of layer 4. They are filled with the clasts and disaggregated grains of host rocks. The original stratifications of the clastic dikes are locally convex upwards (Fig. 9C) suggesting slow upward escape of the internal fluid. The slumps, thrust, and clastic dikes presumably formed by the overlying flow of the Tayu Volcaniclastic Bed F or subsequent mass movement of the Tayu Volcaniclastic Bed F on a northward-dipping slope.

Sedimentary processes

The Tayu Volcaniclastic Bed E is interpreted as a subaqueous mass-flow deposit of coarse pumice and non- to poorly vesiculated glassy clasts. This deposit contains no evidence of a high-temperature emplacement, and a subaqueous depositional setting is indicated by load casts, water-escape structures, rip-up blocks of shale, and the lithofacies association with marine black shales.

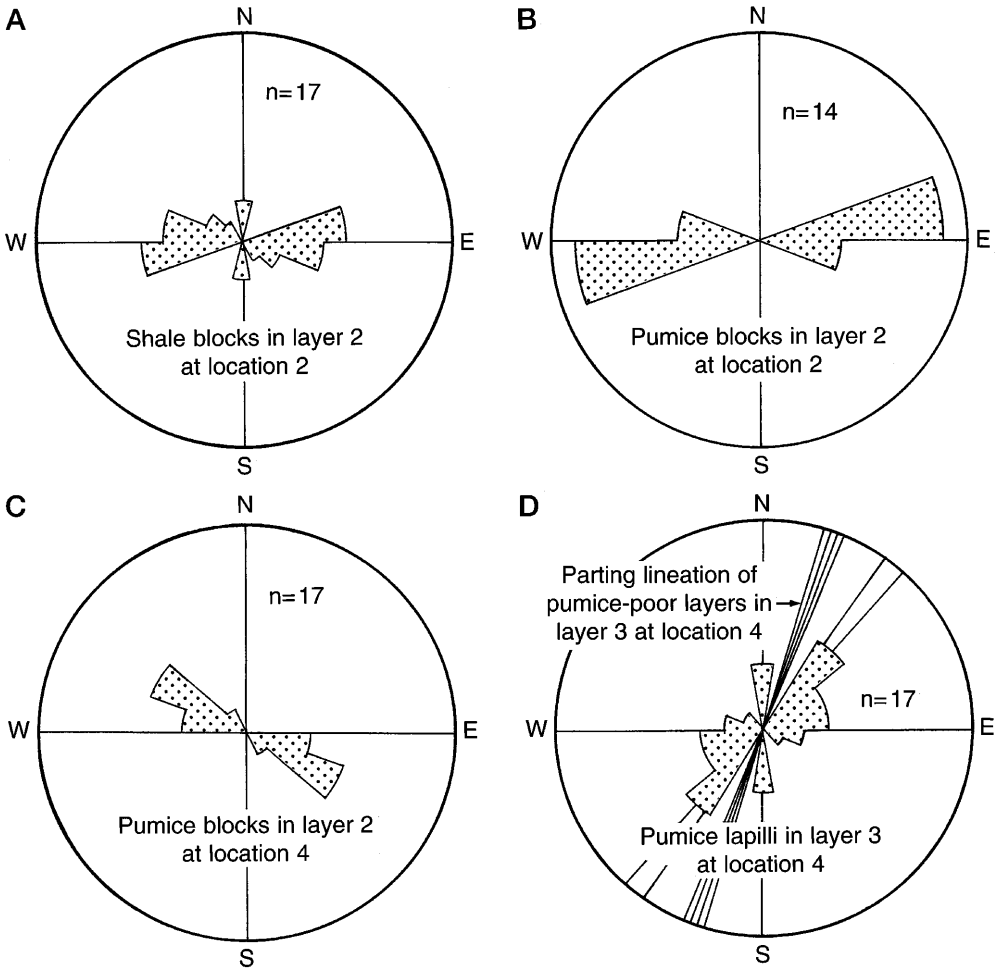

Fig. 7A–D Orientation of the long axes of shale blocks and pumice blocks and lapilli, and orientation of parting lineation. The orientation data sets (**A–D**) were collected from the points *a–d* shown in Fig. 2

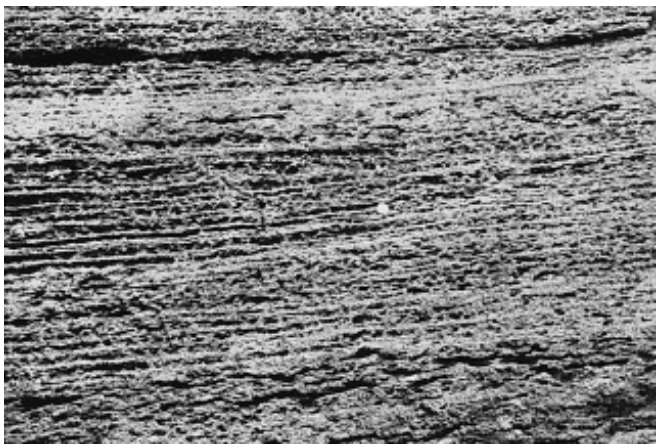

Fig. 8 Horizontally interbedded pumice-rich and pumice-poor layers of layer 3 at location 4. *Lens cap* is 6 cm in diameter

Upward fining and upward depletion of lithic clasts, and upward concentration of pumice clasts with depletion of fine ash component, indicate that the mass flow responsible for the Tayu Volcaniclastic Bed E was fluidized and expanded, thus enabling sedimentary processes to sort the material.

Sediment support mechanisms

In fluidized and expanded flows, the fall velocity and response to dispersive pressure of sediment clasts vary according to their size and bulk density. The size of coexisting vesicular and non-vesicular clasts of different densities may therefore provide an opportunity to test the mechanism of sediment support (e.g. Cole and Stanley 1994). If the constituent clasts have been supported by suspension and deposited grain by grain from the suspension load, coexisting clasts of different densities and sizes are equivalent in falling velocity and their equivalent diameters can be calculated according to the following equation for the terminal fall velocity U of a particle of density ρ_s and diameter D_s in a fluid of density ρ_f:

$$U = K\{4D_s(\rho_s - \rho_f)g/3C_d\rho_f\}^{1/2}, \quad (1)$$

where K is a dimensionless settling coefficient variable with particle shape and to be 1 for sphere, and g is the acceleration due to gravity. C_d is a dimensionless drag coefficient, variable with the Reynolds number,

$$Re = \rho_f U D_s/\mu_f, \quad (2)$$

where μ_f is the viscosity of fluid (Allen 1984, pp 75–82). Cashman and Fiske (1991) calculated the terminal fall

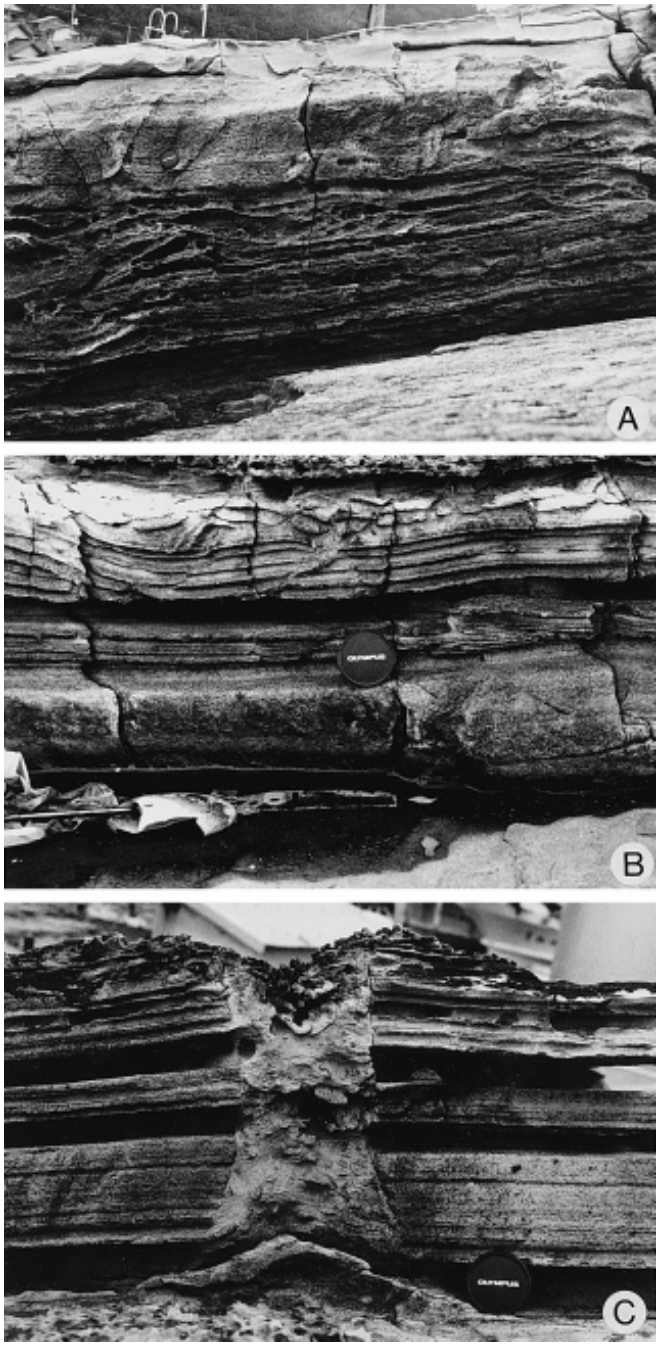

Fig. 9A–C Features of layer 4 at location 4. **A** Dune or antidune-like stratifications transitional to parallel stratifications. **B** Minor thrusts at the top. **C** Clastic dike extending to the overlying pumice lapilli tuff of the Volcaniclastic Bed F. *Lens cap* diameter is 6 cm

velocities in water for pumice and lithic clasts of a wide range of diameter and bulk density by using Eqs. (1) and (2) with the assumption that

$$K = 1 \tag{3}$$

and

$$C_d = 24/Re \text{ at } 0.5 < Re < 750 \tag{4}$$

and

$$C_d = 0.445 \text{ at } 750 < Re < 3.5 \times 10^5. \tag{5}$$

The curves, however, cannot apply to coarse clasts of block size. Instead, when particles 1 and 2 of densities ρ_1 and ρ_2 and diameters D_1 and D_2 fall at the same velocity in a fluid of density ρ_f, and K and C_d are constant irrespective of Re or D_s, we have a simple relationship between the two particles from Eq. (1):

$$D_1/D_2 = (\rho_2 - \rho_f)/(\rho_1 - \rho_f). \tag{6}$$

On the other hand, if they have been supported by dispersion (clast-to-clast collision), the diameter ratio of the coexisting clasts of different densities is inversely proportional to the square root of their density ratio (Sallenger 1979):

$$D_1/D_2 = (\rho_2/\rho_1)^{1/2}. \tag{7}$$

In the case of the Tayu Volcaniclastic Bed E, the pumice and lithic clasts are too intensely altered and lithified to be disaggregated into individual clasts for measuring their sizes. The mean of the long diameters of ten coarsest clasts, however, can be easily obtained on the outcrops. The original densities of the pumice and lithic clasts are also uncertain because of intense alteration and compaction, but could be estimated indirectly. Pumice clasts in the Tayu Volcaniclastic Bed E, which are mainly coarse lapilli to fine blocks in size, have a porosity larger than 60–70%. By assuming the density of such felsic glass to be 2.3 g/cm^3 (e.g. Fisher 1965), the bulk densities of the dry and water-saturated pumice clasts are therefore estimated to be smaller than 1 and 1.6 g/cm^3, respectively. These values suggest that the pumice clasts were water-saturated prior to their deposition and deposited with a density ranging from 1 to 1.6 g/cm^3. Coexisting non-vesicular lithic clasts are plagioclase-phyric glassy rhyolite, and minor crystalline volcanic rocks and clastic rocks. Thus, their mean density may be 2.5 g/cm^3, slightly denser than volcanic glass.

Figure 10 shows the plots of the long diameters of ten coarsest pumice clasts and ten coarsest lithic clasts in the Tayu Volcaniclastic Bed E at location 4. The data from layer 3 and the upper parts of the minor flow units of layer 2 cluster around the line calculated by using Eq. (6) with $\rho_{\text{pumice}} = 1.3$ g/cm^3 (an intermediate value of the estimated range, and equivalent to a porosity of 76%), $\rho_{\text{lithic}} = 2.5$ g/cm^3, and $\rho_{\text{water}} = 1$ g/cm^3. On the other hand, the data from layer 1 and the lower parts of the minor flow units of layer 2, where lithic clasts are concentrated or inversely graded, cluster around the line calculated by using Eq. (7) with the same set of the densities, or disperse between the two lines (Fig. 10). Layer 3 and the upper parts of the minor flow units of layer 2 are therefore interpreted as the deposits from sediment loads supported mainly by suspension, whereas layer 1 and the lower parts of the minor flow units of layer 2 by dispersion or both dispersion and suspension. Although shape and size of sediment particle and

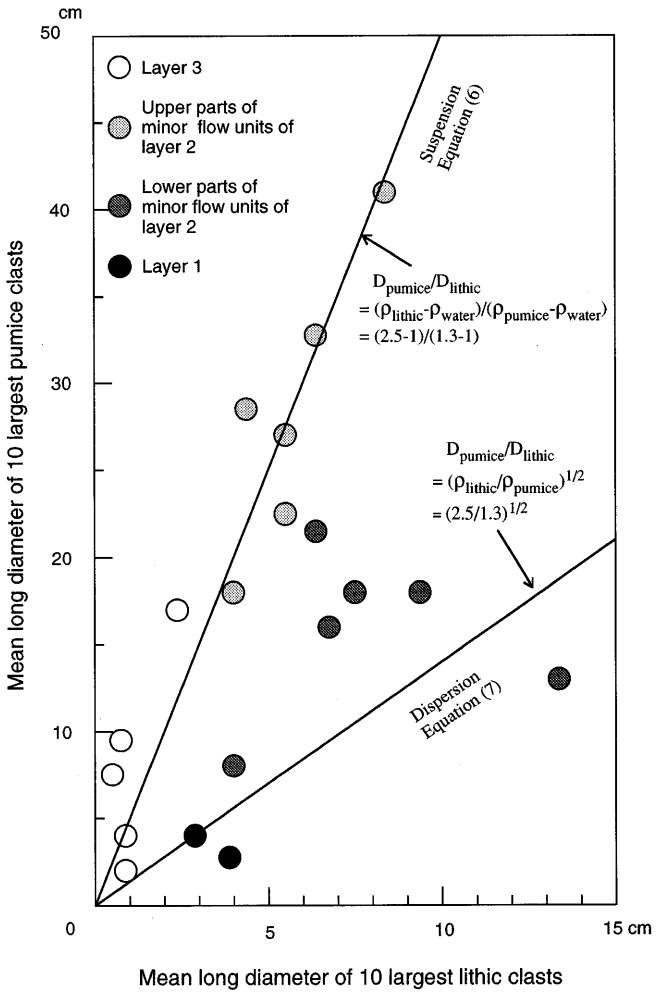

Fig. 10 Relationship between the diameters of ten coarsest pumice and lithic clasts at location 4

particle concentration are important constraints on the hydrodynamic behaviors of solid particles (Komar and Reimer 1978; Sallenger 1979; Lowe 1988; Cashman and Fiske 1991), this interpretation is supported by sedimentary facies as discussed below.

Mode of sedimentation

Inverse grading of lithic clasts in the basal part of layer 1 can be generated in a lithic-concentrated sheared flow, either because dispersive pressure is greatest for coarser clasts (Bagnold 1956) or because finer clasts can filtrate downward between coarser clasts (Middleton 1970). Basal folding (Fig. 3B) suggests large shear stresses developed during deposition of the inversely graded part of layer 1. Shale blocks in this layer are likely to have been torn off from the underlying mud beds and carried upward by the shear stress developed within the flow (Kano and Takeuchi 1989).

Normal grading of lithic clasts in the upper part of layer 1 represents fallout of denser, coarser clasts from suspension load. Layer 1 is interpreted to have been deposited from a gravelly high-density turbulent flow. Lag breccias (Druitt and Sparks 1982), which commonly occur in the basal part of proximal to medial subaerial ash-flow deposits (Druitt and Sparks 1982; Walker 1985; Wilson 1985; Freundt and Schmincke 1985, 1986; Druitt and Bacon 1986; Suzuki-Kamata and Kamata 1990), can also be similarly deposited (Druitt and Bacon 1986).

Undulation of the upper surface of layer 1 with E–W trending crests normal to the flow direction indicates that shear stresses were important even at the beginning of deposition of layer 2. The large shear developed within the flow would allow shale rip-up blocks to be uplifted and form the swarms in layer 2 (Figs. 4 and 5). Northward thinning of layer 1 with concordant thickening of layer 2 (Fig. 2) and gradual depletion of fine ash probably occur by gravitational segregation of the clasts of different densities and sizes in the cohesionless turbulent flow.

Layer 2 and its minor depositional units are similar in size- and compositional grading to many subaerial ash-flow deposits (Sparks et al. 1973; Fisher 1979; Sheridan 1979; Wilson 1985) or the massive lower division of those subaqueous volcaniclastic mass-flow deposits (subaqueous "ash-flow" deposits) believed to have been generated directly from volcanic eruptions (Fiske and Matsuda 1964; Niem 1977; Carey and Sigurdsson 1980; Fisher 1984; Cousineau 1994). Traction structures, however, are more common, due presumably to coarse clast size and development of large shear stresses.

The lower part of each minor depositional unit is similar in internal features to layer 1, which is a lithic-rich deposit from alternating traction and suspension loads. Local stratification in the basal part suggests a large frictional drag developed along the basal part of the turbidite. On the other hand, the upper part is likely a deposit from the remaining more pumiceous part of the sediment load. Coarse pumice clasts are buoyant in the gravelly lower part of the flow, and within a turbulent flow, lift forces arising from the flow-velocity gradient developed and from proximity of bed (Allen 1984, pp 85–88) are expected to act on coarse clasts (Kano and Takeuchi 1989). Coarse pumice clasts could therefore be uplifted to the levels where the total upward force balances with the weight, and could come to lie in swarms with the long axes parallel to the layer or unit boundaries and normal to the flow direction (Figs. 6 and 7).

The internal minor depositional units of layer 2 might reflect repeated flow transformations (Fisher 1983), which occur commonly by incorporation of ambient fluids at the flow head or due to abrupt changes of topography (Fisher 1984; Freundt and Schmincke 1985, 1986; Nemec 1990). Alternatively, they represent the deposits from crossing of flow lobes or unsteady eruption processes which generated the original flow. Entrainment of water into the flow head and the result-

ing flow inflation will cause deceleration of the flow front and allow the dense underflow to proceed ahead (Huppert et al. 1986). If water ingestion by the flow head and sediment supply to the depositional flow boundary are unsteady, this gravity-driven process may repeat many times, with progressively thinner flows bifurcating into even thinner offspring resulting in the minor depositional units of layer 2. The seafloor topography is unlikely to change significantly within a few hundred meters. Other possibilities, such as unsteady eruptions or crossing of flow lobes, however, cannot be excluded.

Layer 3 is interpreted to have been deposited from the remaining lithic-poor, pumiceous turbulent flow. Pumice-poor layers are laminated representing deposition from traction loads. On the other hand, pumice-rich layers show no distinct grading and probably represent rapid deposition from suspension. The preferential alignment of pumice lapilli parallel to the flow direction can be attributed to the internal shear in a rapidly flowing suspension load or the shear imparted from the overlying flow during the final stages of deposition. Layer 3 is similar in occurrence and grain size population to the doubly graded beds of subaqueous pyroclastic flow deposits (Fiske and Matsuda 1964) and has some analogies with ash-cloud layers of subaerial ash-flow deposits (Sparks et al. 1973; Fisher 1979) presumably reflecting similar modes of transport and deposition. Alternating deposition of pumice-poor and pumice-rich layers could occur through repeated flow transformations in some way similar to layer 2 or strong pulsation of currents (Hiscott 1994).

Layer 4 is comparable to the Bouma divisions of sand turbidites. This layer is well stratified and sorted, with little fine ash. Anti-dune-like wavy or hummocky cross-stratification of this layer may be generated by standing waves along a dense underflow and the overlying, less dense, thicker turbulent flow even in deep water environments (Prave and Duke 1990; Yagishita 1994). The parallel- to wavy-, locally cross-stratified lower part is probably analogous to turbidite divisions b and c, and the parallel-stratified upper part is similar to division d. This type of deposit is similar to the ash turbidites described by Wright and Mutti (1981).

The Tayu Volcaniclastic Bed E may be compared with Lowe's (1982) high-density gravelly to sandy turbidite (Fig. 11). Because of the density differences between the constituent clasts, the same divisions R_2 and R_3 are assigned to layers 1 and 2, and to the internal depositional units of layer 2. Pumice-poor, laminated layers of layer 3 are probably correlated to division S_1, and are transitional to pumice-rich layers in the same layer. The pumice-rich layers appear massive, but are interpreted to represent divisions S_2 and S_3. A high rate of fallout of pumice clasts may have suppressed the development of grading and stratification in the layers.

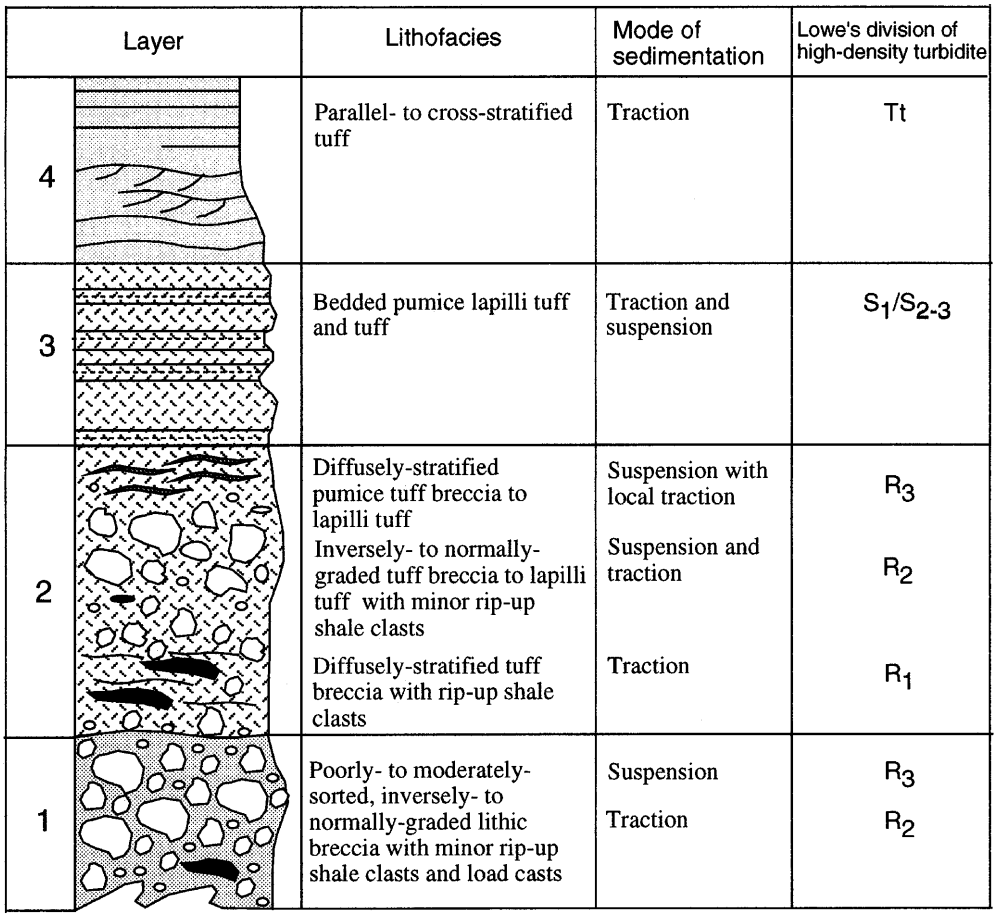

Fig. 11 Idealized sedimentary features of the Tayu Volcaniclastic Bed E, and correlation with the Lowe's (1982) divisions of high-density turbidite. (Not to scale)

Origin of the mass flow

The constituent pumice of the Tayu Volcaniclastic Bed E is much coarser and its lower part is crudely stratified, dissimilar to known deposits of subaqueous pyroclastic flows and volcaniclastic mass flows (Fig. 11). This provides clues to solve the origin of the mass flow deposit, as discussed below.

Source area

The flow direction of the Tayu Volcaniclastic Bed E is from south to north at location 2 and from SSW to NNE at location 4, as inferred from the imbrication of shale blocks and other sedimentary structures (Fig. 7). Similar flow directions are inferred for the overlying and underlying volcaniclastic mass-flow deposits, and therefore the source of the Tayu Volcaniclastic Bed E is likely also a submarine rhyolite volcanic edifice somewhere within the Asahiyama area (Fig. 1). The water depth of the source is uncertain, but might be deep because the contemporaneous argillaceous rocks in the surrounding areas contain benthic foraminiferas indicative of continental shelf to upper bathyal environments, and neither shallow marine fossils nor terrestrial materials.

Origin of coarse pumice

The Tayu Volcaniclastic Bed E comprises pumice blocks and lapilli with a significant amount of non- to poorly vesiculated lapilli and is poor in fine ash. The constituent pumice clasts are highly to extremely vesiculated, similar to pumices of plinian eruptions (Houghton and Wilson 1989). The products of plinian eruptions are, however, normally ash and fine pumice lapilli (e.g. Walker 1980, 1981, 1983), even in subaqueous settings (e.g. Fiske and Matsuda 1964; Niem 1977; Cashman and Fiske 1991; Kokelaar and Busby 1992; Cousineau 1994). Although it is plausible that fine components may have dispersed elsewhere while coarse components settled out to form a mass flow, the Tayu Volcaniclastic Bed E is much coarser than subaqueous "ash-flow" deposits. On the other hand, a significant amount of coarse lapilli and blocks may be produced in subaqueous lava fountaining, but these are poorly to moderately vesicular, not pumiceous in the strict sense (Mueller and White 1992). Coarse pumice clasts might therefore be produced by eruption of a highly vesicular magma at high ambient pressures in deep water, with a small excess pressure of vesicle-filling fluids and partial fragmentation of vesicular magma (R. S. Fiske, pers. commun.). The eruption could occur due to either vesiculation of the magma as it rises within the conduit or to explosive collapse of lava, plausibly associated with phreatomagmatic explosions. Non- to poorly vesiculated glassy clasts associated with coarse pumice clasts may represent a quenched crust of the magma either extruding over the vent or plugging the conduit. Subaqueous "plinian" eruptions, which produce highly vesiculated finer clasts, occur presumably at shallower water depths or with more volatile-rich magmas.

Coarse lapilli and blocks of pumice accumulated thick in the submarine caldera floor and flank of Myojin Knoll, Izu-Ogasawara Arc (Yuasa 1995), are thought to represent an example of pyroclastic eruption in deep water (R. S. Fiske, pers. commun.). The coarse pumice deposits exposed on the caldera wall are well sorted, and are massive at water depths of 1140 to 650 m and stratified at water depths of 650 to 590 m. Pumice blocks up to 1–2 m in length are dispersed on the top surface of the deposits 590 m deep below sea level (Yuasa 1995).

Subaqueous and subglacial felsic lavas are enclosed usually by a glassy, dense quenched rim in direct contact with water or ice. Their inner part, especially where close to the quenched crust, is commonly pumiceous due to the gas exsolution and growth of vesicles, with the vesicles stretched by flowage of the lava (Yamagishi and Dimroth 1985; Kano et al. 1991; Furnes et al. 1980), similar to subaerial ones (Eichelberger et al. 1986; Fink and Manley 1989; Fink et al. 1992). In subaerial cases the pumiceous zone is approximately 10% of the total volume (e.g. Fink and Manley 1989; Fink et al. 1992). In deep water volatile escape from magma is suppressed by the high water pressure, and a thicker pumiceous zone may develop (G. J. Orton, pers. commun.). Some subaqueous lava domes are in fact associated with large amounts of well-vesiculated hyaloclastites spalled off from the domes (Kurokawa 1991). However, it is still under debate whether an entire lava can vesiculate to form a permeable foam (Eichelberger et al. 1986; Wesrich and Eichelberger 1994) or cannot (Fink et al. 1992). In any case the pumiceous zone explodes when its pressure exceeds the strength of the crust. The source of this explosion is restricted mainly to the pumiceous zone, and therefore the products are mainly clasts of pumice with a significant amount of non- to poorly vesiculated glassy clasts. Some subaerial pyroclastic flows are known to have been produced in this way (Fink and Manley 1989).

A lava may also explode due to generation of steam from water incorporated into its midst or trapped beneath the lava from the interstitial water of the underlying rocks (Shephered and Sigurdsson 1982). Gravitational collapse of the lava may also cause small explosions (Sato et al. 1992). The two types of explosions commonly generate mass flows of hot lava clasts (e.g. Rose et al. 1977; Swanson et al. 1987; Sato et al. 1992; Yamamoto et al. 1993). In these cases a large amount of lithics is produced as observed for many block- and ash-flow deposits (e.g. Mellors et al. 1988; Sato et al. 1992).

It is known in subaqueous settings that coarse pumice clasts reaching ten and several meters in length are produced upon subaqueous gravity collapse of thermally stressed and cracked pumiceous carapace of lava

dome. The coarse pumice clasts are usually found as isolated "fallout" clasts on the sediments of the surrounding areas (Mahood 1980; Clough 1981, 1982; Wilson and Walker 1985). In a submarine eruption from Kikai caldera, Japan, numerous hot pumice blocks of meter size floated on the sea for a while before sinking block by block upon cooling (Tanakadate 1935), and were found to be sparsely distributed on the caldera floor in a subsequent submersible survey (Nakamura et al. 1986). Hot pumice clasts ejected into water have a larger chance to reach the water surface in proportion to their size, because pumice clasts are buoyant as long as they are sufficiently hot to generate vapor films on their surfaces (Tanakadate 1935; Whitham and Sparks 1986). Once they have reached the water surface, they become buoyant for weeks or months as their pores are filled with the air upon cooling (Whitham and Sparks 1986), whereas some others sink due to invasion of water into the hot interiors upon fracturing by thermal stress-induced contraction or volatile expansion (Tanakadate 1935; R. S. Fiske, pers. commun.). Hence, many pumice blocks float away from the source and sink sporadically (Mahood et al. 1980; Clough et al. 1981, 1982; Kato 1987). Hot pumice clasts erupted into the air and emplaced on the water surface are also unlikely to form mass flows for the same reason.

Generation of the mass flow

As discussed above, the coarse fibrous pumice debris of the Tayu Volcaniclastic Bed E stems probably from a deep submarine, explosive eruption of vesicular magma or explosive collapse of lava. Intense shear in the basal part of the Tayu Volcaniclastic Bed E may reflect rapid lateral movement of the coarse clasts fallen out from an eruption plume.

As shown in an illustration of a story of explosive collapse of lava (Fig. 12A) and succeeding generation of a mass flow (Fig. 12B), a subaqueous pyroclastic eruption plume should involve a low and wide gas thrust region due to a high ambient pressure (Kokelaar and Busby 1992), and is normally expected to collapse easily by water entrainment to form water-logged mass flows (Kano et al. 1996). The resulting mass flow must therefore, be dense with a large lateral momentum. When the mass flow travels down the slope of the volcanic edifice, some coarse hot pumice blocks will reach the water surface and float away together with the finer materials blown upwards by explosion or lifted by upward thermal convection (Cashman and Fiske 1991). Some portion of the eruption products, however, may continue to flow downslope as hot pumice clasts become denser by ingesting water and disintegrate into finer clasts due to thermal stress-induced strain and/or grain-to-grain collision. This is similar to what happens as pyroclastic flows enter shallow water (Kano 1990) or travel down subaqueous slopes (Cole and DeCelles 1991; Kano et al. 1994).

Alternatively, coarse pumiceous clasts emplaced on a subaqueous slope may subsequently slump due to later eruptions, earthquakes, tsunamis, storms, or other catastrophic events, similar to the collapse of marine, dome-top pumiceous tuff cone (Cas et al. 1990 and references therein). Water-saturated pumice blocks will be close to or only slightly larger than water in bulk density, and can be mobilized by even small external forces. Moving downslope, the slumping pyroclastic mass evolves probably to a sediment gravity flow (Middleton and Hampton 1973) with progressive dilution and fluidization through water ingestion.

In either case the resulting deposit will contain little evidence of high-temperature emplacement with similar internal structures. This makes it difficult to specify the origin of the deposits of this type. This author, however, believes that the Tayu Volcaniclastic Bed E was formed during an eruption because of (a) thick accumulation of homogeneous and unique composition, (b) predominance of internal shear, (c) absence of fossils

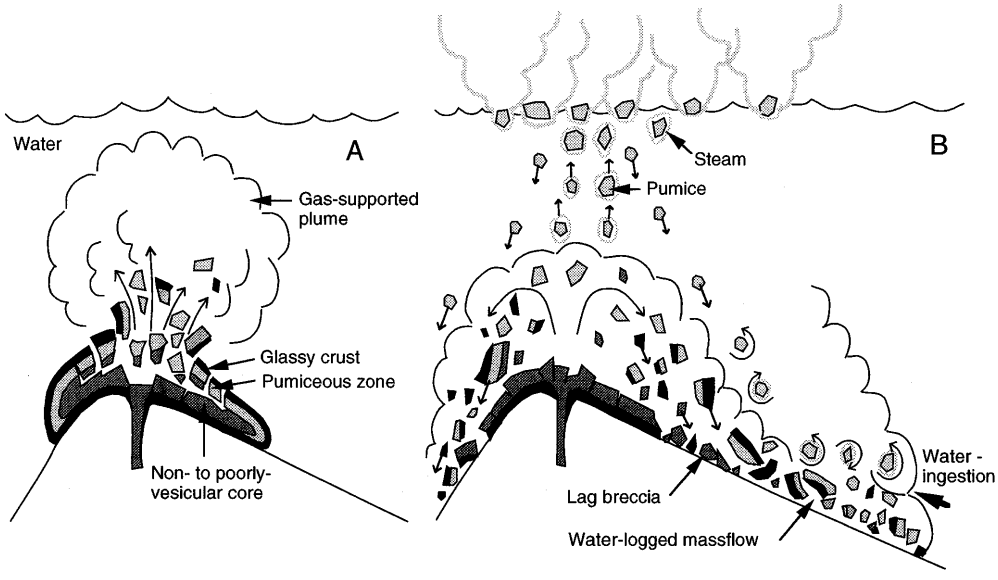

Fig. 12 A model for generation of (**B**) a coarse mass flow by (**A**) subaqueous explosion of a lava. (Not to scale)

and normal sediments in between the underlying and overlying volcaniclastic beds, (d) lack of significant abrasion of clasts, and (e) absence of thick piles of coarse pumice debris in the inferred source area.

Conclusions

A submarine coarse volcaniclastic mass-flow deposit in the Miocene Josoji Formation, Shimane Peninsula, is interpreted as the product of a deep submarine, explosive eruption of vesicular magma or explosive collapse of lava. The deposit contains no evidence of emplacement at high temperature, but could have been formed during an eruption.

Acknowledgements This work was supported financially by the program of the Geological Survey of Japan for regional geologic mapping in the east Shimane Prefecture, and considerably benefitted from long discussions with G. J. Orton. Critical comments by T. Ui, E. Yamada, T. Yamamoto, H. Hoshizumi, and F. Masuda were instructive. The manuscript was improved considerably by the comments of G. J. Orton as well as journal reviewers, R. S. Fiske and C. J. Busby. G. J. Orton suggested the importance of internal shear in interpretation of depositional and eruptive processes. R. S. Fiske kindly encouraged me to discuss eruption styles which might produce coarse pumice clasts.

References

Allen JRL (1984) Sedimentary structures. Their characteristic and physical basis, vol 1. Depelopments in Sedimentology 30. Elsevier, Amsterdam

Bagnold RA (1956) The flow of cohesionless grains in fluid. Phil Trans Royal Soc London A242:235–297

Carey SN, Sigurdsson H (1980) The Roseau Ash: deep-sea tephra deposits from a major eruption on Dominica, Lesser Antilles Arc J Volcanol Geotherm Res 7:67–86

Cas RAF, Wright JV (1987) Volcanic successions. Allen and Unwin Ltd, London

Cas RAF, Wright JV (1991) Subaqueous pyroclastic flows and ignimbrites: an assessment. Bull Volcanol 53:357–380

Cas RAF, Allen RL, Bull SW, Clifford BA, Wright JV (1990) Subaqueous, rhyolitic dome-top tuff cones: a model based on the Devonian Bunga Beds, southern Australia and a modern analogue. Bull Volcanol 52:159–174

Cashman KV, Fiske RS (1991) Fallout of pyroclastic debris from submarine volcanic eruptions. Science 253:275–280

Clough BJ, Wright JV, Walker GPL (1981) An unusual bed of giant pumice in Mexico. Nature 289:49–50

Clough BJ, Wright JV, Walker GPL (1982) Morphology and dimensions of the young comendite lavas of La Primavera volcano, Mexico. Geol Mag 119:477–485

Cole RB, DeCelles PG (1991) Subaerial to submarine transitions in early Miocene pyroclastic flow deposits, southern San Joaquin basin, California. Geol Soc Am Bull 103:221–235

Cole RB, Stanley RG (1994) Sedimentology of subaqueous volcaniclastic sediment gravity flows in the Neogene Santa Maria Basin, California. Sedimentology 41:37–54

Cousineau PA (1994) Subaqueous pyroclastic deposits in an Ordovician for-arc basin: an example from the Saint-Victor Formation, Quebec Appalachians, Canada. J Sediment Petrol A64:867–880

Druitt TH, Bacon CR (1986) Lithic breccia and ignimbrite erupted during the collapse of Crater Lake Caldera, Oregon. J Volcanol Geotherm Res 29:1–32

Druitt TH, Sparks RSJ (1982) A proximal ignimbrite breccia facies on Santorini, Greece. J Volcanol Geotherm Res 13:147–171

Eichelberger JC, Carrigan CR, Westrich HR, Price RH (1986) Non-explosive silicic volcanism. Nature 323:598–602

Fink JH, Manley CR (1989) Explosive volcanic activity generated from within advancing silicic lava flows. In: Latter JH (ed) Volcanic hazard. IAVCEI Proceeding in Volcanology 1. Springer, Berlin Heidelberg New York, pp 169–179

Fink JH, Anderson SW, Manley CR (1992) Textural constraints on effusive silicic volcanism: beyond the permeable foam model. J Geophys Res 97:9073–9083

Fisher RV (1965) Settling velocity of glass shards. Deep Sea Res 12:345–353

Fisher RV (1979) Models of pyroclastic surges and pyroclastic flows. J Volcanol Geotherm Res 6:305–318

Fisher RV (1983) Flow transformations in sediment gravity flows. Geology 11:273–274

Fisher RV (1984) Submarine volcanic rocks. In: Kokelaar BP, Howells MF (eds) Marginal basin geology. Geol Soc Lond Spec Publ 16:5–27

Fisher RV, Schmincke H-U (1984) Pyroclastic rocks. Springer, Berlin Heidelberg New York

Fiske RS (1963) Subaqueous pyroclastic flows in the Ohanapecosh Formation, Washington. Geol Soc Am Bull 74:391–406

Fiske RS, Matsuda T (1964) Submarine equivalents of ash flows in the Tokiwa Formation, Japan. Am J Sci 262:76–106

Francis EH, Howells MF (1973) Transgressive welded ash-flow tuffs among the Ordovician sediments of NE Snowdonia, North Wales. J Geol Soc Lond 129:621–641

Freundt A, Schmincke H-U (1985) Lithic-enriched segregation bodies in pyroclastic flow deposits of Laacher See Volcano (East Eifel, Germany). J Volcanol Geotherm Res 25:193–224

Freundt A, Schmincke H-U (1986) Emplacement of small-volume pyroclastic flows at Laacher See (East Eifel, Germany). Bull Volcanol 48:39–59

Furnes H, Friedleifsson IB, Atkins FB (1980) Subglacial volcanics – on the formation of acid hyaloclastites. J Volcanol Geotherm Res 8:95–110

Hiscott RN (1994) Traction-carpet stratification in turbidites – fact or fiction? J Sediment Res A 64:204–208

Houghton BF, Wilson CJN (1989) A vesicularity index for pyroclastic deposits. Bull Volcano 51:451–462

Howells MF, Campbell SDG, Reedman AJ (1985) Isolated pods of subaqueous welded ash-flow tuff: a distal facies of the Capel Curig Volcanic Formation (Ordovician). Geol Mag 122:175–180

Huppert HE, Turner JS, Carey SN, Sparks RSJ, Hallworth MA (1986) A laboratory simulation of pyroclastic flows down slopes. J Volcanol Geotherm Res 30:179–199

Kano K (1990) An ash-flow tuff emplaced in shallow water, Early Miocene Koura Formation, southwest Japan. J Volcanol Geotherm Res 40:1–9

Kano K, Nakano S (1986) Geology of the Etomo district. With Geological Sheet Map at 1:50000. Geol Surv Japan, 30 pp (in Japanese with English abstract)

Kano K, Takeuchi K (1989) Origin of mudstone clasts in turbidites of the Miocene Ushikiri Formation, Shimane Peninsula, Southwest Japan. Sediment Geol 62:79–87

Kano K, Nakano S, Mimura K (1988) Deformation structures in shale bed indicate flow direction of overlying Miocene subaqueous pyroclastic flow. Bull Volcanol 50:380–385

Kano K, Takeuchi K, Yamamoto T, Hoshizumi H (1991) Subaqueous rhyolite block lavas in the Miocene Ushikiri Formation, Shimane Peninsula, SW Japan. J Volcanol Geotherm Res 46:241–253

Kano K, Orton GJ, Kano T (1994) A hot Miocene subaqueous scoria-flow deposit in the Shimane Peninsula, SW Japan. J Volcanol Geotherm Res 60:1–14

Kano K, Yamamoto T, Ono K (1996) Subaqueous eruption and emplacement of the Shinjima Pumice, Shinjima (Moeshima) Island, Kagoshima Bay, SW Japan. J Volcanol Geotherm Res (in press)

Kato Y (1987) Woody pumice generated with submarine eruption. J Geol Soc Japan 77:193–206
Kato I, Muroi I, Yamazaki T, Abe M (1971) Subaqueous pyroclastic flow deposits in the Upper Donzurubo Formation, Nijo-San district, Osaka, Japan. J Geol Soc Japan 77:193–206
Kokelaar BP, Busby CJ (1992) Subaqueous explosive eruption and welding of pyroclastic deposits. Science 257:196–201
Komar PD, Reimer CE (1978) Grain shape effects on settling rate. J Geol 86:193–209
Kurokawa A (1991) Formation of felsic pumiceous hyaloclastites: a case study from Tadami district, Fukushima Prefecture, Japan. J Mineral Petrol Econ Geol (GANKO) 86:439–458 (in Japanese with English abstract)
Lajoie J (1979) Volcaniclastic rocks. In: Walker RG (ed) Facies models. Geoscience Canada Reprint Ser 1, Geol Soc Canada, pp 191–200
Lowe DR (1982) Sediment gravity flows: II. Depositional models with special reference to the deposits of high-density turbidity currents. J Sediment Petrol 52:279–297
Lowe DR (1988) Suspended-load fallout rate as an independent variable in the analysis of current structures. Sedimentology 35:765–776
Mahood GA (1980) Geological evolution of a Pleistocene rhyolitic center – Sierra La Primavera, Jalisco, Mexico. J Volcanol Geotherm Res 8:199–230
Mellors RA, Waitt RB, Swanson DA (1988) Generation of pyroclastic flows and surges by hot-rock avalanches from the dome of Mount St. Helens volcano, USA. Bull Volcanol 50:14–25
Middleton GV (1970) Experimental studies related to problems of flysch sedimentation. In: Lajoie J (ed) Flysch sedimentology in North America. Geol Assoc Can Spec Paper 7:253–272
Middleton GV, Hampton MA (1973) Sediment gravity flows: mechanics of flow and deposition. In: Middleton GV, Bouma AH (eds) Turbidites and deep water sedimentation. Soc Econ Paleontol Mineral Pacific Sect, pp 1–38
Mueller WM, White JDL (1992) Felsic fire-fountaining beneath Archean sea: pyroclastic deposits of the 2730 Ma Hunter Mine Group, Quebec, Canada. J Volcanol Geotherm Res 54:117–134
Nakamura K-I, Sakaguchi K, Nagai T (1986) Marine geological survey in the Kikai caldera with special references to the occurrence of giant pumices, the detailed survey on topography and the measurement of sea water temperature. Tech Rep Japan Marine Sci and Technol Center, Spec Issue of the 2nd Symposium on Deep Sea Research Using the Submersible "Shinkai 2000" System, pp 137–155 (in Japanese with English abstract)
Nemec W (1990) Aspect of sediment movement on steep delta slopes. Spec Publ Int Ass Sediment 10:29–73
Niem AR (1977) Mississipian pyroclastic flow and ash-fall deposits in the deep-marine Ouachita flysch basin, Oklahoma and Arkansas. Bull Geol Soc Am 88:49–61
Nomura R (1986) Geology of the central part in the Shimane Peninsula, part 2. Biostratigraphy and paleoenvironment viewed from benthic foraminifera. J Geol Soc Japan 92:461–475 (in Japanese with English abstract)
Prave AR, Duke WL (1990) Small-scale hummocky cross-stratification in turbidites: a form of antidune stratification? Sedimentology 37:531–539
Rose WI Jr, Pearson T, Bonis S (1977) Nue'e ardente eruption from the foot of a dacite lava flow, Santiago volcano, Guatemala. Bull Volcanol 40:1–16
Sallenger AH Jr (1979) Inverse grading and hydraulic equivalence in grainflow deposits. J Sediment Petrol 49:553–562
Sato H, Fujii T, Nakada S (1992) Crumbling of dacite dome lava and generation of pyroclastic flows at Unzen volcano. Nature 360:664–666
Schneider J-L, Fourquin C, Paicheler J-C (1992) Subaqueously welded ash-flow tuffs: the Visean of southern Vosges (France) and the Upper Cretaceous of northern Anatolia (Turkey). J Volcanol Geotherm Res 49:365–383
Shephered JB, Sigurdsson H (1982) Mechanism of the 1979 explosive eruption of Soufriere volcano, St. Vincent. J Volcanol Geotherm Res 17:1–29
Sheridan MF (1979) Emplacement of pyroclastic flows: a review. In: Chapin CE, Elston WE (eds) Ash-flow tuffs. Geol Soc Am Spec Paper 180:125–136
Spars RSJ, Self S, Walker GPL (1973) Products of ignimbrite eruption. Geology 1:115–118
Stix (1991) Subaqueous, intermediate to silicic-composition explosive volcanism: a review. Earth Sci Rev 31:21–53
Suzuki-Kamata K, Kamata H (1990) The proximal facies of the Tosu pyroclastic-flow deposits erupted from Aso Caldera, Japan. Bull Volcanol 52:325–333
Swanson DA, Dzurisin D, Holcomb RT, Iwatsubo EY, Chadwick WW Jr, Casadevall TJ, Ewert JW, Heliker CC (1987) Growth of the lava dome at Mount St. Helens, Washington, (USA), 1981–1983. In: Fink JH (ed) The emplacement of silicic domes and lava flows. Geol Soc Am Spec Paper 212:1–16
Tamura Y, Koyama M, Fiske RS (1991) Paleomagnetic evidence for hot pyroclastic debris flow in the shallow submarine Shirahama Group (Upper Miocene–Pliocene), Japan. J Geophys Res 96, B 13:21779–21787
Tanakadate S (1935) Preliminary report of the eruption of Iwojima, Kagoshima Prefecture. Bull Volcanol Soc Japan (Ser 1) 2:188–209 (in Japanese)
Tasse N, Lajoie J, Dimroth E (1978) The anatomy and interpretation of an Archean volcaniclastic sequence, Noranda region, Quebec. Can J Earth Sci 15:874–888
Walker GPL (1980) The Taupo pumice: product of the most powerful known (ultraplinian) eruption? J Volcanol Geotherm Res 8:69–94
Walker GPL (1981) Plinian eruptions and their products. Bull Volcanol 44:223–240
Walker GPL (1983) Ignimbrite types and ignimbrite problems. J Volcanol Geotherm Res 17:65–88
Walker GPL (1985) Origin of coarse lithic breccias near ignimbrite source vents. J Volcanol Geotherm Res 25:157–171
Westrich HR, Eichelberger JC (1994) Gas transport and bubble collapse in rhyolitic magma: an experimental approach. Bull Volcanol 56:447–458
Wilson CJN (1985) The Taupo eruption, New Zealand. II. The Taupo ignimbrite. Phil Trans Royal Soc Lond A314:229–310
Wilson CJN, Walker GPL (1985) The Taupo eruption, New Zealand. I. General aspects. Phil Trans Royal Soc Lond A314:199–228
Whitham AG, Sparks RSJ (1986) Pumice. Bull Volcanol 48:209–223
Wright JV, Mutti E (1981) The Dali Ash, Island of Rhodes, Greece: a problem in interpreting submarine volcanogenic sediments. Bull Volcanol 44:153–167
Yamagishi H, Dimroth E (1985) A comparison of Miocene and Archean rhyolite hyaloclastites: evidence for a hot and fluid rhyolite lava. J Volcanol Geotherm Res 23:337–355
Yagishita K (1994) Antidunes and traction-carpet deposits in deep-water channel sandstones, Cretaceous, British Columbia, Canada. J Sediment Res A64:34–41
Yamada E (1973) Subaqueous pumice flow deposits in the Onikobe Caldera, Miyagi Prefecture, Japan. J Geol Soc Japan 79:589–597
Yamada E (1984) Subaqueous pyroclastic flows: their development and their deposits. In: Kokelaar BP, Howells MF (ed) Marginal basin geology. Geol Soc Lond Spec Publ 16:29–35
Yamamoto T, Takarada S, Suto S (1993) Pyroclastic flows from the 1991 eruption of Unzen volcano, Japan. Bull Volcanol 55:166–175
Yamazaki T, Kato I, Murai I, Abe M (1973) Textural analysis and flow mechanism of the Donzurubo subaqueous pyroclastic flow deposits. Bull Volcanol 37:231–244
Yuasa M (1995) Myojin Knoll, Izu-Ogasawara Arc: submersible study of submarine pumice volcano. Bull Volcanol Soc Japan 40:277–284 (in Japanese with English abstract)